High breakdown voltage AlGaN/GaN HEMTs with a dipole layer for microwave power applications

Jiangfeng Du ✉, *Xiaoyun Li, Zhiyuan Bai, Yong Liu, Qi Yu*

State Key Laboratory of Electronic Thin Films and Integrated Devices, University of Electronic Science and Technology of China, Chengdu 610054, People's Republic of China
✉ *E-mail: jfdu@uestc.edu.cn*

Published in Micro & Nano Letters; Received on 13th September 2018; Revised on 3rd January 2019; Accepted on 15th January 2019

A novel high breakdown voltage AlGaN/GaN high electron mobility transistor with a dipole layer (GaN DL-HEMT) is proposed in this work. The dipole layer (DL) is formed by AlGaN which is attached to the AlGaN barrier and located in the passivation layer between drain and gate electrodes. DL can improve significantly the breakdown voltage (BV) by modulating the distribution of electric field along the channel. The proposed GaN DL-HEMT exhibits a high BV of 1130 V, which increased from 496 V of conventional GaN HEMT with gate–drain distance of 5 μm, while on-state resistance keeps 0.48 Ω.mm and FOM at a high level of 2.67 GW/cm^2 is obtained. Meanwhile, the cutoff frequency maintains a large value as high as 32.4 GHz, which increases by 74% compared with GaN with a gate field plate. The novel GaN DL-HEMT shows great prospects in microwave power applications.

1. Introduction: AlGaN/GaN high electron mobility transistors (HEMTs) have drawn intensive attention for high frequency and high voltage applications due to its wide band gap and high saturation velocity properties [1]. However, there are still some issues such as electric field concentration at drain-side edge of the gate, which limit the breakdown voltage (BV). In general, the technique of multiple field plates (FP) is adopted to manage the distribution of surface electric field in GaN HEMTs [2, 3]. However, the processing of multiple FP is difficult [2–4] and FP structure will increase the parasitic capacitance, which results in the degradation of high-frequency performance of the device [5, 6]. In addition, doping Fe/C in GaN buffer layer [7, 8] is also one of the feasible solutions for breakdown enhancement. However, subsequently introducing impurity scattering may make the other performances of GaN HEMT deteriorating [9, 10]. It is important to improve the BVs and keep low on-state resistances and frequency characteristics at the same time for GaN HEMT used in microwave power applications. Recently, a dipole layer (DL) model had been proposed [11–13], which was composed of two charged surfaces. Each surface of the layer has an equal and opposite surface-charge density compared with one another, and the surface charges were lying close and paralleling to each other. Kubicek *et al.* had demonstrated the formation of DL at the high-k/SiO_2 interface and applied to CMOS [11, 12]. Fireman *et al.* had applied DL on an InAlN/GaN interface and achieved rectifying dipole diodes with excellent performance [13]. However, few researches about introducing DL in GaN HEMT have been reported.

In this Letter, we proposed a GaN HEMT with a dipole layer structure (GaN DL-HEMT). The DL is formed by unintentional doped AlGaN which is attached to the AlGaN barrier and is located in the passivation layer between gate and drain electrodes. Compared to conventional GaN HEMT, the DL can form negative charges along the interface of $Al_xGa_{1-x}N/Al_{0.28}Ga_{0.72}N$ DL barrier [14]. So by partly depleting 2DEG in channel layer, the DL modulates the distribution of electric field along the channel, which results in a great enhancement of the BV. Different from FP and buffer doping technology, the proposed GaN DL-HEMT could obtain high BV significantly and keep low on-state resistances and frequency characteristics at the same time, which portends its great prospects in microwave power applications.

2. Device structure and simulation models: The schematic cross-section of the proposed GaN DL-HEMT is shown in Fig. 1. The device structures and characteristics have been simulated by TCAD using Silvaco and the model used in this simulation include the Shockley–Read–Hall model (SRH), Fermi–Dirac statistics, the polarisation model, Albrecht mobility model and Selberherr impact ionisation model. The effects of charging and discharging of traps are calculated by the SRH model. In the simulation, all calculations are based on the Fermi–Dirac statistics. Besides, according to the work of Albrecht *et al.*, mobility model is chosen [15]. The POLARIZ model in ATLAS is used to calculate the polarisation at the AlGaN/GaN heterojunctions [16]. The total polarisation is calculated by

$$P_{\mathrm{t}} = P_{\mathrm{sp}} + P_{\mathrm{pi}} \tag{1}$$

where P_{sp} is the spontaneous polarisation, which is given by the material parameters of AlN and GaN in ATLAS. The spontaneous polarisation of $Al_xGa_{1-x}N$ is given by

$$P_{\mathrm{sp}}(Al_xGa_{1-x}N) = x.P_{\mathrm{sp}}(AlN) + (1-x)P_{\mathrm{sp}}(GaN) \tag{2}$$

P_{pi} is the piezoelectric polarisation, which is given by

$$P_{\mathrm{pi}} = 2\frac{as-a0}{a0}\left(e31 - \frac{c13}{c33}e33\right) \tag{3}$$

where C_{13} and C_{33} are the elastic constants, and e_{31} and e_{33} are the piezoelectric constants. For AlGaN/GaN heterojunctions, $a_s$and a_0 are the average value of the lattice constant of GaN and AlGaN, and a_0 is calculated by Vegard's law [17]. Table 1 shows the value of parameters in the simulation.

The Selberherr's impact ionisation model was used to simulate the device breakdown. The following expressions show the impact ionisation coefficients for electrons (α_n) and holes (α_p) [16]:

$$\alpha_n = a_n \exp\left[-\left(\frac{b_n}{E}\right)^m\right] \tag{4}$$

doi: 10.1049/mnl.2018.5556

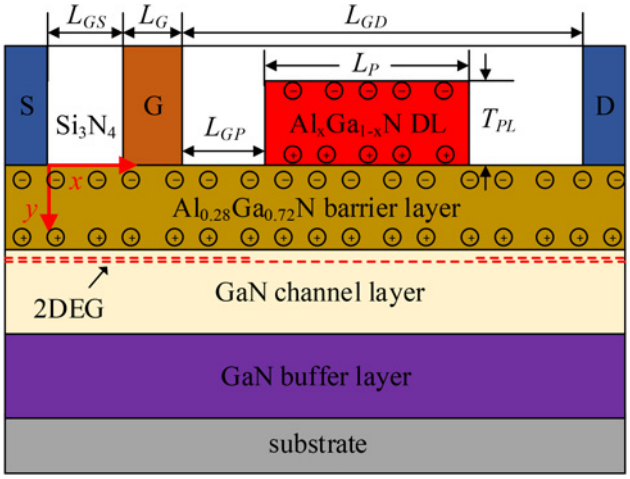

Fig. 1 *Schematic cross-section of GaN DL-HEMT*

Table 1 Material parameters of AlN and GaN [16]

Parameters captions	Paramet-ers	Units	GaN	AlN
piezoelectric const. (z)	e_{33}	C/m^2	0.67	1.5
piezoelectric const. (x, y)	e_{31}	C/m^2	−0.34	−0.53
lattice constant	a_0	Å	3.189	3.112
spontaneous polarisation	P_{sp}	C/m^2	−0.034	−0.09

$$\alpha_p = a_p \exp\left[-\left(\frac{b_p}{E}\right)^m\right] \tag{5}$$

The electric field in the direction of current flow at a particular position in the structure is described as E and the parameters are set as $a_n = a_p = 1.1438 \times 10^7$ cm^{-1}, $b_n = b_p = 23.8933$ MV/cm and $m = 1$ [18]. Table 2 shows the device parameters used in this Letter.

Fig. 2 shows the electron concentration distribution and the 2DEG density of GaN DL-HEMT and the conventional GaN HEMT at $V_{GS} = 0$ V, $V_{DS} = 0$ V, respectively. In Figs. 2*a* and *b*, σ_1, σ_2 and σ_3 are the polarisation charges of $Al_xGa_{1-x}N$, $Al_{0.28}Ga_{0.72}N$ and GaN, respectively. According to the formula (2), the spontaneous polarisation of the AlGaN increases by increasing the Al_{mol}. Due to the difference of spontaneous polarisation intensity between $Al_xGa_{1-x}N/Al_{0.28}Ga_{0.72}N$ $(0 < x < 0.28)$ DL barrier, there will induce some negative charges along the interface of $Al_xGa_{1-x}N/Al_{0.28}Ga_{0.72}N$ DL barrier [14]. These negative charges at the DL/AlGaN barrier interface will impact the electric potential distribution of the barrier layer to increase the effective barrier height, which will lower the concentration of 2DEG in the region, forming a structure of low-density drain [19]. Analogously, the DL structure such as the high-k/SiO_2 interface or the other polar materials/AlGaN interface can also influence device characteristics in the same way [11–13]. In order to better present the DL principle, the DL is formed by unintentional doped AlGaN in this structure.

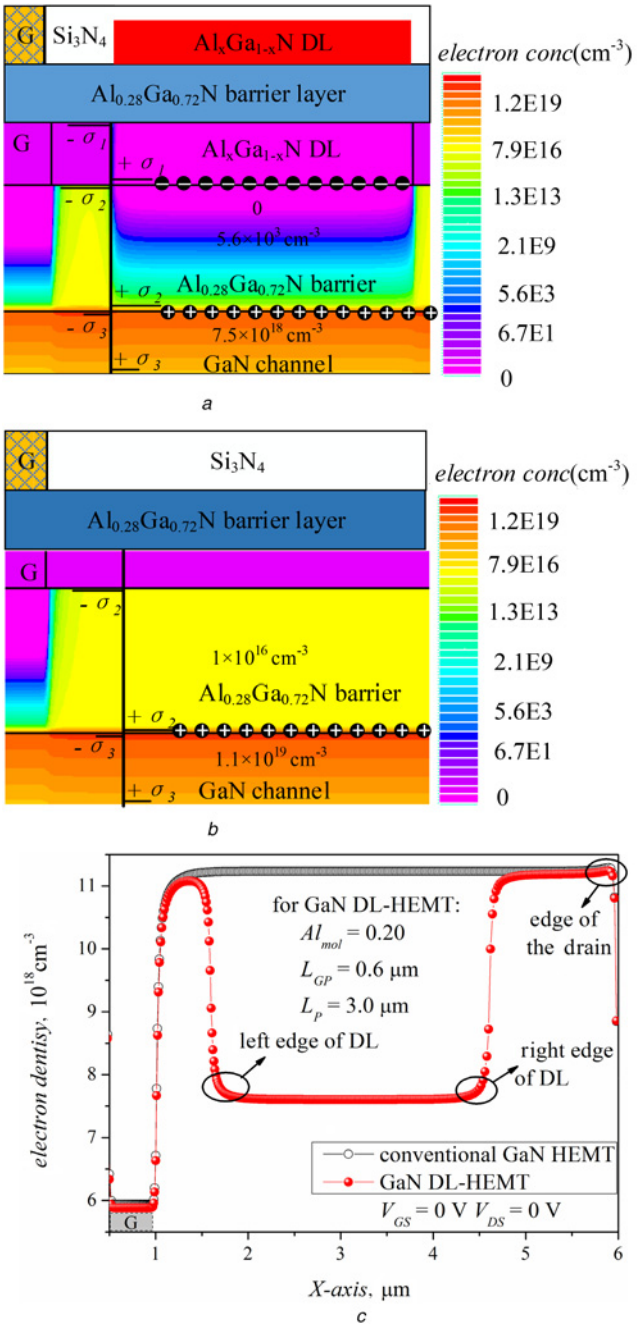

Fig. 2 *Off-state electron concentration distributions of*
a GaN DL-HEMT
b Conventional GaN HEMT at $V_{GS} = 0$ V, $V_{DS} = 0$ V, where σ_1, σ_2 and σ_3 are the polarisation charges of $Al_xGa_{1-x}N$, $Al_{0.28}Ga_{0.72}N$ and GaN
c Electron distribution along the channel for a GaN DL-HEMT and conventional GaN HEMT

Table 2 GaN DL-HEMT device specifications

Parameters	Units	Values	Parameter captions
L_G	μm	0.5	gate length
L_S	μm	0.5	source length
L_D	μm	0.5	drain length
L_{GD}	μm	5	distance between gate and drain
L_{GS}	μm	0.5	distance between gate and source
T_{PL}	nm	10	DL thickness
T_{buf}	μm	1	GaN buffer layer thickness
T_{AlGaN}	nm	20	AlGaN barrier layer thickness
T_P	nm	200	passivation layer thickness

Fig. 3 shows horizontal electric field distribution along the channel of conventional GaN HEMT, GaN FP-HEMT and GaN DL-HEMT, and the vertical electric field distribution of GaN DL-HEMT crossing the bipolar layer to the channel is shown in the inserted figure. Obviously, for conventional GaN HEMT, one peak can be seen at drain-side edge of the gate

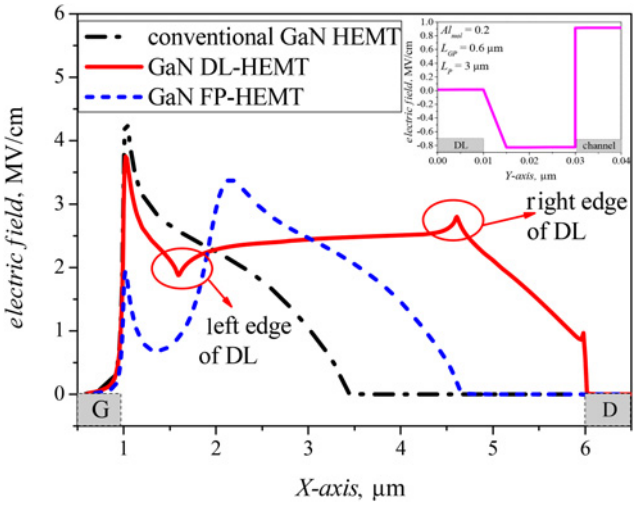

Fig. 3 *Horizontal electric field distribution along the channel of optimised GaN DL-HEMT compared with conventional GaN HEMT and GaN FP-HEMT. Insert: vertical electric field distribution of GaN DL-HEMT crossing the bipolar layer to channel (x = 3.0 μm)*

($x = 0$), and along with positive direction of X-axis, the value of electric field strength declines drastically. For GaN FP-HEMT with the length of FP (L_{FP}) of 2 μm, two peaks can be seen at both sides of FP structure. Nevertheless, the problem of uneven distribution of electric field exists. For GaN DL-HEMT, there exists the second higher peak with high electric field strength at the drain-side edge of the DL besides the peak at drain-side edge of the gate. On the other hand, due to the decrease of electric field at right of the drain-side edge of gate and at left of gate-side edge of DL, a lowest peak of electric field will appear, but still at a high level. The vertical electric field of GaN DL-HEMT is much lower than the theoretical limit of GaN material. So compared with the conventional GaN HEMT and GaN FP-HEMT, GaN DL-HEMT of electric field distribution is more uniform and the peak of electric field strength is lower than the conventional GaN HEMT, portending that the proposed device has better BV blocking capability.

3. Results and discussion: The simulated output characteristics of conventional GaN HEMT and GaN DL-HEMT are shown in Fig. 4, and the inserted figure shows transfer characteristics ($V_{DS} = 15$ V) of conventional GaN HEMT and GaN DL-HEMT. In the simulation

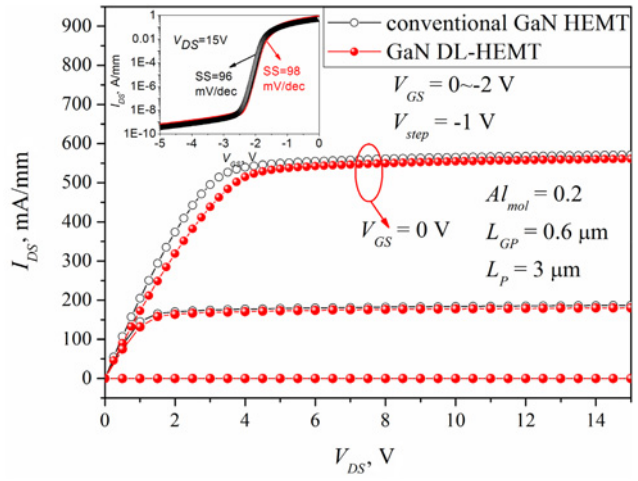

Fig. 4 *Output characteristics of conventional GaN HEMT and GaN DL-HEMT. Insert: transfer characteristics ($V_{DS} = 15$ V) of conventional GaN HEMT and GaN DL-HEMT*

of output characteristics for GaN DL-HEMT, Al_{mol}, L_{GP} and L_P are set to 0.2, 0.6 μm and 3.0 μm, respectively. For conventional GaN HEMT and GaN DL-HEMT, the maximum saturation current density (I_{DSmax}) is 571 and 561 mA/mm at $V_{GS} = 0$ V. According to the expression of I_{DSsat} [20]

$$I_{DSsat} = \frac{\beta}{2}(V_{GT} - R_S I_{DSsat})^2 \quad (6)$$

The on-state saturation current is mainly related to the gate–source series resistance and is independent of the gate–drain series resistance. As shown in Fig. 2*c*, since the DL is placed in the passivation layer between the gate and drain, the distribution of 2DEG in the channel is mainly influenced in this region resulting in the gate–drain series resistance decreasing but the gate–source series resistance not be affected. So the on-state saturation current of GaN DL-HEMT and the conventional GaN HEMT is close. At the same time, by calculating the specific R_{on} of the two structures at $V_{GS} = 0$ V, the R_{on} of the GaN DL-HEMT is 0.48 mΩ.cm^2, and the value of R_{on} for GaN DL-HEMT increases slightly compared to 0.41 mΩ.cm^2 of conventional GaN HEMT. R_{on} of GaN DL-HEMT still remains lower than R_{on} of other reported GaN HEMTs [21]. Besides the transfer characteristics and the subthreshold slope (SS) are acquired at $V_{DS} = 15$ V. The SS of DL-HEMT and GaN HEMT are both at a same level of 100 mV/Dec.

For conventional GaN HEMT, the BV is 496 V in this simulation, which is in keeping with an experimental result of 510 V using same device parameters [22]. For GaN DL-HEMT, Al_{mol}, L_{GP} and L_P determine the value of BV.

The Al_{mol} determines the polarisation and depletion ability of the DL structure, which would greatly impact the BV, I_{DSmax} and R_{on} of the device. Fig. 5 shows the relationship of BV, FOM, R_{on} in GaN DL-HEMT with $L_{GP} = 0$ μm, $L_P = 2$ μm, and the inserted figure shows electron distribution along the channel with different Al_{mol} for GaN DL-HEMT at $V_{GS} = 0$ V, $V_{DS} = 0$ V. As shown in Fig. 5, with the increase of Al_{mol}, BV decreases slowly at the first and decreases sharply after the $Al_{mol} = 0.25$, and R_{on} decreases continuously and always at a low level. To acquire the optimum polarisation effect, the Al_{mol} of 0.28 in AlGaN barrier layer is chosen and the optimised Al_{mol} of DL was set as 0.20 in this device. The higher value of BV (1020 V) and higher FOM (2.26 GW/cm^2) was acquired.

We optimised the position of the DL. Fig. 6 shows the relationship of BV and L_{GP} for GaN DL-HEMT. As shown in Fig. 6, FP-HEMT can obtain the highest BV when $L_{FP} = 2$ μm, and the optimal value is only 665 V, which is in keeping with an

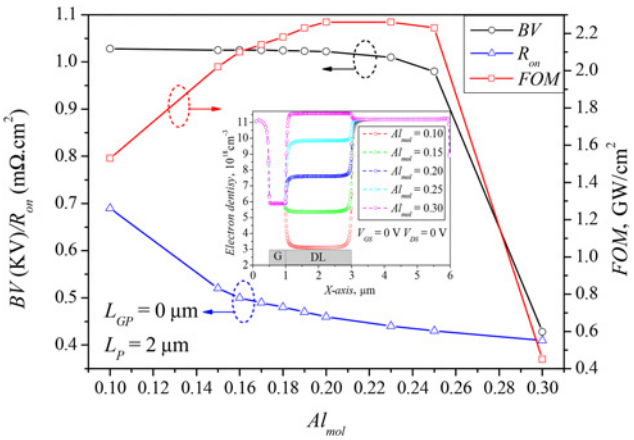

Fig. 5 *Relationship of Al_{mol} and BV, FOM, R_{on} in GaN DL-HEMT. Insert: electron distribution along the channel with different Al_{mol} at $V_{GS} = 0$ V, $V_{DS} = 0$ V*

doi: 10.1049/mnl.2018.5556

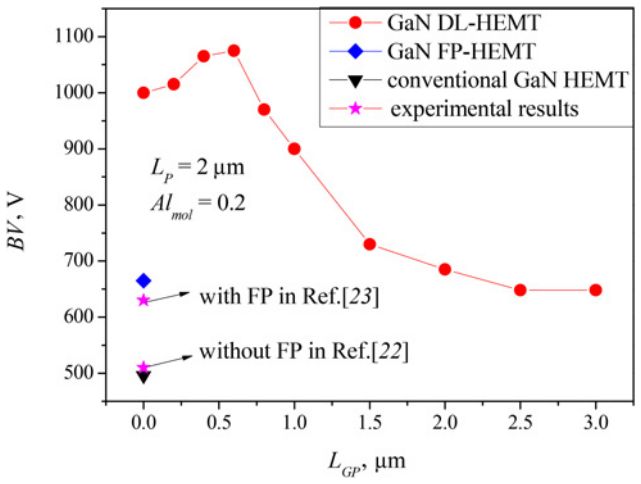

Fig. 6 *Relationship of L_{GP} and BV in GaN DL-HEMT*

experimental result of 630 V [23]. For GaN DL-HEMT (Al_{mol} = 0.2, L_P = 2 μm), the BV increases first and then decreases sharply with the increase of L_{GP}, and the highest value of BV (1075 V) is obtained at L_{GP} = 0.6 μm. Due to the uniformity of the electric field distribution, BV decreases. DL structure will lose the ability of modulating electric field along the gate edge when DL is far away from the drain-side edge of gate.

The relationship of BV, R_{on} and FOM with L_P are shown in Fig. 7. As shown in Fig. 7, when L_P is small, the depletion region broadens with L_P gradually increases, and average electric field strength is increased, thus BV of the device is improved. When L_P reaches 3 μm, the uniformity of electric field is optimal and the optimum of BV is 1130 V. However, if L_P is continuously increased, the peak electric field of the drain edge of the DL will decline, so the uniformity of electric field will deteriorate, thus BV of the device is decreased. As can be seen in Fig. 7, when L_P = 3 μm the devices processed to get the maximum FOM (2.67 GW/cm^2) and BV (1130 V).

We analysed the frequency characteristics of GaN DL-HEMT, FP-HEMT and the conventional GaN HEMT in the same simulation models and the cutoff frequency (f_T) as a function of V_{GS} for the three structures is shown in Fig. 8. The inserted figure shows the C-V simulation results of GaN DL-HEMT, FP-HEMT and the conventional GaN HEMT. f_T of conventional GaN HEMT is 34.3 GHz at V_{GS} = 0 V, which is in keeping with the previous reports [24, 25]. As FP structure will add the parasitic capacitance obviously, which will make the high-frequency characteristic of the device worse, the f_T of GaN FP-HEMT only reach 18.6 GHz,

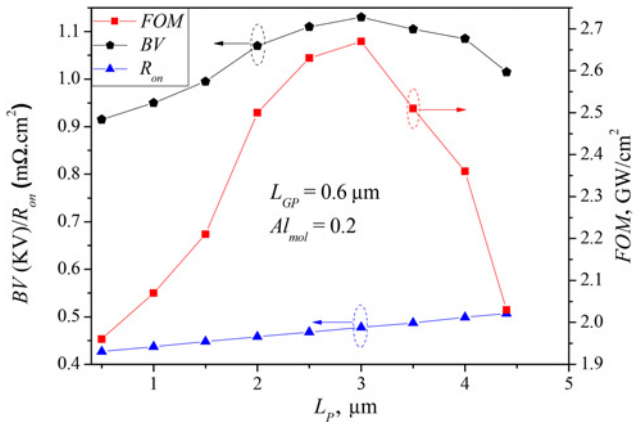

Fig. 7 *Relationship of L_P and BV, FOM, R_{on} in GaN DL-HEMT*

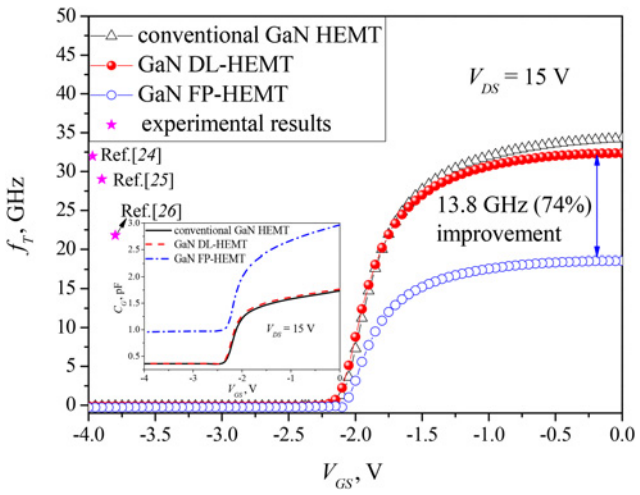

Fig. 8 *Cutoff frequency f_T as a function of V_{GS} for conventional GaN HEMT, GaN DL-HEMT and GaN FP-HEMT. Inset: C-V characteristics of conventional GaN HEMT, GaN DL-HEMT and GaN FP-HEMT*

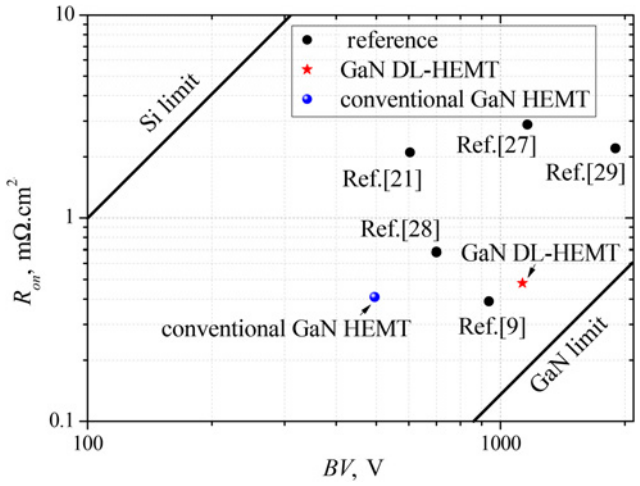

Fig. 9 *Benchmarking the BV and R_{on} of GaN HEMT*

which is consistent with the previous reports [26]. On the other hand, by introducing a DL, f_T of the DL-HEMT can reach 32.4 GHz, which increase by 74% compared with GaN FP-HEMT. Therefore, the GaN DL-HEMT technology can effectively improve the BV and maintain good frequency characteristics.

In Fig. 9, the benchmark plot of BV versus R_{on} for GaN HEMT is shown. A GaN MISHEMT with an 1162 V BV can be achieved with 5 μm field plate which demonstrates a FOM of 0.47 GW/cm^2 [27]. The DH-HEMTs with multiple grating field plates can have a FOM of 0.72 GW/cm^2 with a BV of 700 V [28]. A BV of 1900 V can be achieved by utilising integrated slant field plates in GaN HEMT, which demonstrates a power FOM of 1.6 GW/cm^2 [29]. In this work, the high-performance GaN-HEMT with a DL demonstrates a power FOM as high as 2.67 GW/cm^2 with a BV of 1130 V, which indicates that the device is a promising candidate for power application.

4. Conclusion: In this Letter, we presented high BV GaN-HEMTs with a DL. According to the results of simulation, for GaN DL-HEMT with L_G = 0.5 μm and L_{GD} = 5 μm, a maximum saturation current 561 mA/mm at V_{GS} = 0 V and SS = 98 mV/Dec can be obtained. The devices exhibited great characteristics including a high BV of 1130 V which is 634 V higher than that of the

conventional GaN HEMT and a low on-resistance R_{on} of 0.48 mΩ. cm^2 and a high FOM of 2.67 GW/cm^2. Besides, the f_T of the GaN DL-HEMT maintains a large value as high as 32.4 GHz, which is increased by 74% compared with GaN FP-HEMT. The proposed device with high BV, high frequency and low on-resistance shows great application prospect in microwave power fields.

5. Acknowledgments: This work was financially supported by the National Natural Science Foundation of China under grant no. 61376078.

6 References

[1] Chen K.J., Haberlen O., Lidow A., *ET AL.*: 'GaN-on-Si power technology: devices and applications', *IEEE Trans. Electron Devices*, 2017, **64**, pp. 779–795

[2] Xing H., Dora Y., Chini A., *ET AL.*: 'High breakdown voltage AlGaN-GaN HEMTs achieved by multiple field plates', *IEEE Electron. Device Lett.*, 2004, **25**, pp. 161–163

[3] Dora Y., Chakraborty A., McCarthy L., *ET AL.*: 'High breakdown voltage achieved on AlGaN/GaN HEMTs with integrated slant field plates', *IEEE Electron. Device Lett.*, 2006, **27**, pp. 713–715

[4] Kobayashi K., Hatakeyama S., Yoshida T., *ET AL.*: 'Improved breakdown voltage and RF characteristics in AlGaN/GaN high-electron-mobility transistors achieved by slant field plates', *Appl. Phys. Express*, 2014, **7**, p. 096501

[5] Ahsan S.A., Ghosh S., Sharma K., *ET AL.*: 'Capacitance modeling in dual field-plate power GaN HEMT for accurate switching behavior', *IEEE Trans. Electron Devices*, 2016, **63**, pp. 565–572

[6] Sharma K., Dasgupta A., Ghosh S., *ET AL.*: 'Effect of access region and field plate on capacitance behavior of GaN HEMT'. EDSSC, Singapore, 2015, pp. 499–502

[7] Heikman S., Keller S., DenBaars S.P., *ET AL.*: 'Growth of Fe doped semi-insulating GaN by metalorganic chemical vapor deposition', *Appl. Phys. Lett.*, 2002, **81**, pp. 439–441

[8] Poblenz C., Waltereit P., Rajan S., *ET AL.*: 'Effect of carbon doping on buffer leakage in AlGaNÕGaN high electron mobility transistors', *J. Vac. Sci. Technol.*, 2004, **22**, pp. 1145–1149

[9] Bahat-Treidel E., Brunner F., Hilt O., *ET AL.*: 'Algan/GaN/GaN:C back-barrier HFETs with breakdown voltage of over 1 kV and Low R × A', *IEEE Trans. Electron. Devices*, 2010, **57**, pp. 3050–3058

[10] Uren M.J., Silvestri M., Casar M., *ET AL.*: 'Intentionally carbon-doped AlGaN/GaN HEMTs:necessity for vertical leakage paths', *IEEE Electron. Device Lett.*, 2014, **35**, pp. 327–329

[11] Kirsch P.D., Quevedo-Lopez M.A., Krishnan S.A., *ET AL.*: 'Band edge n-MOSFETs with high-k/metal gate stacks scaled to EOT = 0.9 nm with excellent carrier mobility and high temperature stability'. IEEE Conf., San Francisco, CA, USA, December 2006, pp. 1–4

[12] Kubicek S., Schram T., Paraschiv V., *ET AL.*: 'Low VT CMOS using doped Hf-based oxides, TaC-based metals and Laser-only anneal'. IEEE Conf., Washington, DC, USA, December 2007, pp. 49–52

[13] Fireman M.N., Li H.R., Keller S., *ET AL.*: 'Vertical transport in isotype InAlN/GaN dipole induced diodes grown by molecular beam epitaxy', *J. Appl. Phys.*, 2017, **121**, p. 205702

[14] Ambacher O., Smart J., Shealy J.R., *ET AL.*: 'Two-dimensional electron gases induced by spontaneous and piezoelectric polarization charges in N- and Ga-face AlGaN/GaN heterostructures', *J. Appl. Phys.*, 1999, **85**, pp. 3222–3233

[15] Albrecht J.D., Wang R.P., Ruden P.P., *ET AL.*: 'Electron transport characteristics of GaN for high temperature device modeling', *J. Appl. Phys.*, 1998, **83**, pp. 4777–4781

[16] ATLAS User's Manual.: Silvaco Int., Santa Clara, CA, USA, 2012

[17] Ambacher O., Majewski J., Miskys C., *ET AL.*: 'Pyroelectric properties of Al(In)GaN/GaN hetero- and quantum well structures', *J. Phys. Condens. Matter*, 2002, **14**, pp. 3399–3434

[18] Bulutay C.: 'Electron initiated impact ionization in AlGaN alloys', *Semicond. Sci. Technol.*, 2002, **17**, pp. L59–L62

[19] Marso M., Javorka P., Dikme Y., *ET AL.*: 'Influence of doping concentration on DC and RF performance of AlGaN/GaN HEMTs on silicon substrate', *Phys. Stat. Sol.*, 2003, **200**, pp. 179–182

[20] Daniel D., Nwen T.L.: 'Metal-(n) AIGaAs-GaAs two-dimensional electron gas FET', *IEEE Trans. Electron. Devices*, 1982, **29**, pp. 955–960

[21] Tang Z.K., Jiang Q.M., Lu Y.Y., *ET AL.*: '600-V normally off SiNx/AlGaN/GaN MIS-HEMT with large gate swing and low current collapse', *IEEE Electron. Device Lett.*, 2013, **34**, pp. 1373–1375

[22] Visalli D., Van Hove M., Srivastava P., *ET AL.*: 'Experimental and simulation study of breakdown voltage enhancement of AlGan/GaN heterostructures by Si substrate removal', *Appl. Phys. Lett.*, 2010, **97**, p. 113501

[23] Karmalkar S., Mishra U.K.: 'Enhancement of breakdown voltage in AlGaN/GaN high electron mobility transistors using a field plate', *IEEE Trans. Electron. Devices*, 2001, **48**, pp. 1515–1521

[24] Javorka P., Alam A., Fox A., *ET AL.*: 'High-performance AlGaN/GaN HEMTs on silicon substrates'. IEEE Conf., Smolenice Castle, Slovakia, October 2002, pp. 287–290

[25] Zhou H., Lou X.B., Sutherlin K., *ET AL.*: 'DC and RF performance of AlGaN/GaN/SiC MOSHEMTs with deep sub-micron T-gates and atomic layer epitaxy MgCaO as gate dielectric', *IEEE Electron. Devices Lett.*, 2017, **38**, pp. 1409–1412

[26] Wu Y., Saxler A., Moore M., *ET AL.*: '30-w/mm gan HEMTs by field plate optimization', *IEEE Electron. Device Lett.*, 2004, **25**, pp. 117–119

[27] Zhang Z., Yu G., Zhang X., *ET AL.*: 'Studies on high-voltage GaN-on-Si MIS-HEMTs using LPCVD Si3N4 as gate dielectric and passivation layer', *IEEE Trans. Electron Devices*, 2016, **63**, pp. 731–738

[28] Bahat-Treidel E., Hilt O., Brunner F., *ET AL.*: 'Algan/GaN/AlGaN DH- HEMTs breakdown voltage enhancement using multiple gating field plates (MGFPs)', *IEEE Trans. Electron. Devices*, 2010, **57**, pp. 1208–1216

[29] Dora Y., Chakraborty A., McCarthy L., *ET AL.*: 'High breakdown voltage achieved onAlGaN/GaNHEMTswith integrated slant field plates', *IEEE Electron. Device Lett.*, 2006, **27**, pp. 713–715

doi: 10.1049/mnl.2018.5556